Autohydrolyzed Low-Cost Biomass and Adsorbent Aging

Odysseas Kopsidas

Department of Industrial Management and Technology, University of Piraeus, Piraeus 18534, Greece

Abstract: Autohydrolysis or self-hydrolysis or hydrothermal treatment of lignocellulosic materials like sawdust and straw is already used in bioethanol industry for water soluble fermentable sugars production. The main idea in this paper is the use of the autohydrolysis and other thermochemical treatments' solid residue as an adsorbent. In this study continuous fixed-bed-column systems were investigated. Continue-flow experiments were carried out on stainless steel columns with dimensions 15 × 2.5 and 25 × 2.5 cm. In chemical processing, a packed bed is a hollow tube, pipe, or other vessel that is filled with a packing material.

Key words: Autohydrolysis, adsorption, desorption, biomass, MB (Methylene Blue).

1. Introduction

In fact, the adsorbent is the solid by-product in the fermentable sugars production by autohydrolysis. Autohydrolysis of lignocellulosic materials can be used as a first step while enzymatic or acid hydrolysis is usually used as second step in the bioethanol industry. Many industries, such as paper, plastics, food, printing, leather, cosmetics and textile, use dyes in order to color their products [1]. In textile industries, about 10-15% of the dye gets lost in the effluent during the dyeing process which are harmful products and may cause cancer epidemics [2, 3]. Dyes usually have a synthetic origin and complex aromatic molecular structures which make them more stable and more difficult to biodegrade [1-4]. In wastewater treatment, various methods applied to remove dyes include photocatalytic degradation [5, 6], membrane separation [7], chemical oxidations [8] and electrochemical process. Among the above mentioned techniques of dye removal, the process of adsorption gives the best results as it can be used to remove different types of coloring materials [9]. Adsorption onto activated carbon is the most widespread technology for the removal of pollutants from water and wastewaters.

The adsorbents which authors use are: spruce (*Picea abies*) untreated, spruce modified by autohydrolysis, wheat straw untreated, barley straw untreated, lentil straw untreated, chickpeas straw untreated and algae untreated. The column systems were filed with biomass at various initial dye concentrations, flow rates and bed-depths. The column kinetics of MB (Methylene Blue) adsorption on spruce (*Picea abies*) untreated, spruce modified by autohydrolysis, wheat straw untreated, barley straw untreated, lentil straw untreated, chickpeas untreated, algal untreated biomass, was simulated herein, using biomass as control, in order to facilitate its potential use as a low-cost adsorbent for wastewater dye removal. Economies arise when the facility that can use such adsorption materials is near a source of a lignocellulosic waste as agricultural residues, thus saving transportation cost and contributing to industrial ecology at local level.

2. Materials and Methods

2.1 Materials

The Scots pine (*Pinus sylvestris L.*) sawdust used was obtained from a local furniture manufacturing

---

Corresponding author: Odysseas Kopsidas, Ph.D., research field: environmental economics.

company, as a suitable source for full-scale/industrial applications. The moisture content of the material when received was 8.7% (w/w); after screening, the fraction with particle sizes between 0.2 and 1 mm was isolated. The composition of the raw material was as follows (expressed in % w/w on a dry weight basis): 40.1% cellulose measured as glucan (with 52.5% XRD (X-Ray Diffraction) degree of crystallinity); 28.5% hemicelluloses (16.0% measured as manan, 8.9% measured as xylan and the rest 3.6% measured as arabinan); 27.7% Klason acid-insoluble lignin, 0.2% ash, and 3.5% extractives and other acid soluble components (e.g. acid soluble lignin). The spruce (*Picea Abies*) sawdust used was obtained from a local furniture manufacturing company, as a suitable source for full-scale/industrial applications. The moisture content of the material when received was 9% (w/w); after screening, the fraction with particle sizes between 0.2 and 0.9 mm was isolated. Wheat straw (*Triticum aestivum*) obtained from Thessaly in Central Greece had a moisture content of 8.75% w/w. It was chopped with hedge shears in small pieces and the fraction with sizes 1-2 cm (representing more than 95% of the raw total wheat straw) was collected by sieving. This fraction was chosen because it is more suitable for scale up of the process.

Barley straw (*Hordeum vulgare*) used was obtained from Thessaly (Central Greece), as a suitable source for full-scale/industrial applications. Barley straw contains 27% w/w hemicelluloses, 33% w/w cellulose, lignin 28% w/w and 12% w/w ash. The moisture of the material measured was 8.5% w/w. After grinding in a hummer mill and screening, the fraction with particle sizes between 1 and 2 cm was isolated as "coarse grinded barley straw". The material was saturated for 24 hours prior to adsorption experiments. The moisture of the barley straw was 8.5% w/w. After grinding by a hummer mill and screening, the fraction with particle sizes between 1.5 and 2.5 cm was isolated as "coarse grinded barley straw". It was

saturated for 24 hours before the experimental procedure. The lentil straw (*Lens culinaris*) is an edible pulse. It is a bushy annual plant of the legume family, grown for its lens-shaped seeds. It is about 40 centimeters (16 in.) tall and the seeds grow in pods, usually with two seeds in each. Lentils have been part of the human diet since the aceramic (before pottery) Neolithic times, being one of the first crops domesticated in the Near East. Archeological evidence shows they were eaten 9,500 to 13,000 years ago. Lentil colors range from yellow to red-orange to green, brown and black. Lentils also vary in size and are sold in many forms, with or without the skins, whole or split.

The chickpeas straw is from a plant which grows to between 20-50 cm (8-20 inches) high and has small feathery leaves on either side of the stem. Chickpeas are a type of pulse, with one seedpod containing two or three peas. It has white flowers with blue, violet or pink veins. Chickpeas need a subtropical or tropical climate with more than 400 millimetres (16 in.) of annual rain (citation needed) They can be grown in a temperate climate but yields will be much lower.

Algae (*Microcystis*, *Cyclotella*, *Cryptomonas* and *Scenedesmus*) are a very large and diverse group of simple, typically autotrophic organisms, ranging from unicellular to mu lticellular forms, such as the giant kelp (large brown alga), that may grow up to 50 meters in length. Most are photosynthetic and "simple" because they lack many of the distinct cell organelles and cell types found in land plants. The largest and most complex marine forms are called seaweeds. Wood chips are a medium-sized solid material made by cutting, or chipping, larger pieces of wood. Woodchips may be used as a biomass solid fuel and are raw material for producing wood pulp. They may also be used as an organic mulch in gardening, landscaping, restoration ecology and mushroom cultivation. According to the different chemical and mechanical properties of the masses, the wood logs are mostly peeled, and the bark chips and the

woodchips processed in different processes. Wood chips used for chemical pulp must be relatively uniform in size and free of bark. The optimum size varies with the wood species. It is important to avoid damage to the wood fibres as this is important for the pulp properties. For round wood, it is most common to use disk chippers. A typical size of the disk is 2.0-3.5 m in diameter, 10-25 cm in thickness and weight is up to 30 tons. The disk is fitted with 4 to 16 knives and driven with motors of ½-2 MW. Drum chippers are normally used for wood residuals from saw mills or other wood industry.

MB (CI 52015) is a heterocyclic aromatic chemical compound with the molecular formula $C_{16}H_{18}N_3SCl$. It has many uses in a range of different fields, such as biology and chemistry. At room temperature it appears as a solid, odorless, dark green powder that yields a blue solution when dissolved in water. The hydrated form has 3 molecules of water per molecule of MB. MB should not be confused with methyl blue, another histology stain, new MB, nor with the methyl violets often used as pH indicators. As an experimental pharmaceutical drug, the INN (International Nonproprietary Name) of MB is methylthioninium chloride. MB was first prepared in 1876 by German chemist Heinrich Caro (1834-1910). The formation of MB after the reaction of hydrogen sulfide with dimethyl-p-phenylenediamine and iron(III) at pH 0.4-0.7 is used to determine by photometric measurements sulfide concentration in the range 0.020 to 1.50 mg/L (20 ppb to 1.5 ppm). The test is very sensitive and the blue coloration developing upon contact of the reagents with dissolved H_2S is stable for 60 min. Ready-to-use kits such as the Spectroquant sulfide test [8] facilitate routine analyses. The MB sulfide test is a convenient method often used in soil microbiology to quickly detect in water the metabolic activity of SRB (Sulfate Reducing Bacteria). It should be observed that in this test, MB is a product of reaction and not a reagent.

The addition of a strong reducing agent, such as ascorbic acid, to a sulfide-containing solution is sometimes used to prevent sulfide oxidation from atmospheric oxygen. Although it is certainly a sound precaution for the determination of sulfide with an ion selective electrode, it might however hamper the development of the blue color if the freshly formed MB is also reduced, as described here above in the paragraph on redox indicator.

2.2 Pretreatment

The autohydrolysis process was performed in a 3.75-L batch reactor PARR 4843. The isothermal autohydrolysis time was tai = 0, 10, 20, 30, 40 and 50 min (not including the non-isothermal preheating and the cooling time-periods); the reaction was catalyzed by the organic acids produced by the pine sawdust itself during autohydrolysis at a liquid-to-solid ratio of 10:1; the liquid phase volume (water) was 2,000 mL and the solid material dose (pine sawdust) was 200 g; stirring speed 150 rpm. The reaction ending temperature values were $T = 160$ °C, 200 °C and 240 °C, reached after $t = 42$, 62 and 80 min preheating time values, respectively. The autohydrolysis product was filtered using a Buchner filter with Munktell paper sheet (grade 34/N) to separate the liquid phase from the solid phase. The solid residue was washed with water until neutral pH (the initial filtrate pH was 2.90-4.76 depending on the autohydrolysis severity). The solid residue was dried at 110 °C for 10 days at room temperature to reach the humidity of the untreated material. Then it was used as adsorbent.

2.3. Continuous Fixed-Bed Column Studies

Continue-flow experiments were carried out on stainless steel columns with dimensions 15 × 2.5 and 25 × 2.5 cm. The bed height was $x = 15$ cm and 25 cm, respectively. The adsorbent weight was $m = 32$ g and 54 g, respectively. The pH was 8.0. The flow rates were fixed at approximately 20 and 40 mL·min^{-1} using a preparative HPLC (High Performance Liquid Chromatography) pump, LaPrep P110-VWR-VWR

International. The initial concentrations of MB were 160, 80 and 40 mg·L^{-1}. To determine the concentration of MB in the effluent, samples of outflow were peaked at 100 mL intervals. At the end of each one of the above mentioned sorption experiments, desorption tests were performed using distilled water as influent. The flow rate was fixed at about 20 mL·min^{-1}. To determine the concentration of MB in the effluent, samples of outflow were collected at 100 mL intervals.

3. Results and Discussion

3.1 Continuous Fixed-Bed-Column Adsorption Model

A widely used continuous fixed-bed-column model was established by Bohart and Adams, who assumed that the rate of adsorption is controlled by the surface binding (through chemical reaction or physical interaction) between adsorbate and unused capacity of the solid, i.e., adsorption rate = KCC_u, where K is the adsorption rate coefficient, C is the adsorbate concentration at the solid phase at distance x, and C_u is the unused surface adsorptive capacity at time t, expressed as mass per volume of bed. The material balance for adsorbate is given by the partial differential equation:

$$\frac{\partial C_u}{\partial t} = -K \cdot C \cdot C_u \qquad (1)$$

while the corresponding partial differential equation for the C_u decrease is

$$\frac{\partial C}{\partial x} = -\frac{K}{u} \cdot C \cdot C_u \qquad (2)$$

where u is the superficial liquid velocity. These equations are obtained neglecting diffusion and accumulation terms, with assumptions that are valid in chemical engineering practice, provided that strict scale up specifications are kept in the design stage and successful operation conditions are kept in the industrial operation stage.

The differential equations can be integrated over the total length x of the bed to give:

$$\ln\left(\frac{C_i}{C} - 1\right) = \ln[\exp\left(\frac{K.N.x}{u}\right) - 1] - K \cdot C_i \cdot t \quad (3)$$

where N (mg·L^{-1}); is the initial or total adsorption capacity coefficient, also quoted as $C_{u,0}$ [9, 10]; $C =$ effluent concentration (mg·L^{-1}); $C_i =$ influent concentration (mg·L^{-1}); $K =$ adsorption rate coefficient ($L \cdot mg^{-1} \cdot min^{-1}$); $x =$ bed depth (cm); $u =$ linear velocity (cm·min^{-1}); and $t =$ time (min). Since $\exp(K.N.x/u)$ is usually much greater than unity, this equation can be simplified to:

$$\ln\left(\frac{C_i}{C} - 1\right) = \frac{K \cdot N \cdot x}{u} - K \cdot C_i \cdot t \qquad (4)$$

which is commonly used by researchers, because of its convenience in estimating the values of parameters K and N through linear regression either of $\ln[(C_0/C_i) - 1]$ vs. t or t vs. x when the following rearrangement is adopted:

$$t = \frac{N \cdot x}{C_i \cdot u} - \frac{1}{K \cdot C_i} \cdot \left(\ln\frac{C_i}{C} - 1\right) \qquad (5)$$

In this rearrangement, t is the time to breakthrough, i.e., the time period required for concentration to reach a predetermined value. For using the last expression as a linear regression model, wastewater is passed through beds of varying depths, keeping constant C_i and u, preferably at values similar to those expected to prevail under real conditions at full scale. Alternatively, it can be performed by the aid of at least three columns arranged in series. In such a case, sampling takes place at the bottom of each column and is measured for adsorbate concentration, making more frequent measurements when approaching the breakthrough concentration C. Finally, the time at which the effluent reaches this concentration is used as the dependent variable while x plans the role of the independent one. Evidently, the use of such a regression model implies the additional error of measuring the independent variable with less precision

in comparison with the dependent. The common error in both models comes from the estimation of concentration from measuring adsorbance although the reference relation/curve has been structured/drawn in the inverse mode, i.e., for predetermined concentrations the corresponding adsorbances have been measured.

In the present work, the model of Eq. (5) has been used for parameter values estimation through linear regression to obtain numerical results compared with corresponding data found for other fixed bed adsorption studies in literature. The non-linear form of this model is:

$$C = \frac{C_i}{1 + Ae^{-rt}} \qquad (6)$$

where $A = e^{K \cdot N \cdot x / u}$; $r = K \cdot C_i$.

On the other hand, Clark has advanced the Bohart and Adams model by incorporating the parameter n of the Freundlich adsorption isotherm:

$$C = \left[\frac{C_i^{n-1}}{1 + Ae^{-rt}} \right]^{\frac{1}{n-1}} \qquad (7)$$

where n = inverse of the slope of the Freundlich isotherm. Finally, the Bohart and Adams model can be reduced for $n = 2$ from Clark model.

3.2 Continuous Fixed-Bed-Column Desorption Model

The kinetic equation used for desorption is Eq. (8):

$$C = C'_0 \, e^{-k' \cdot t'} \qquad (8)$$

where C'_0 is the initial MB concentration of desorption effluent, k' is desorption rate constant assuming first order desorption kinetics and t' is desorption time.

3.3 Fixed-Bed Column Results for MB Adsorption on Lignocellulosic Biomass

The packing can be randomly filled with small objects like Raschig rings or else it can be a specifically designed structured packing. Packed beds may also contain catalyst particles or adsorbents such as zeolite pellets, granular activated carbon, etc.. The purpose of a packed bed is typically to improve contact between two phases in a chemical or similar process. Packed beds can be used in a chemical reactor, a distillation process, or a scrubber, but packed beds have also been used to store heat in chemical plants. In this case, hot gases are allowed to escape through a vessel that is packed with a refractory material until the packing is hot. Air or other cool gas is then fed back to the plant through the hot bed, thereby pre-heating the air or gas feed. The Ergun equation can be used to predict the pressure drop along the length of a packed bed given the fluid velocity, the packing size, and the viscosity and density of the fluid.

The values of parameters A and r according to the Bohart and Adams model were estimated by LRA (Linear Regression Analysis) from the column effluent data for all the cases. The expressions used to calculate the parameter K and N values after having performed LRA are $K = r/C_i$ and $N = u \, lnA/(xK) = C_i u \, lnA/(xr)$. The effluent dye solution volume V (in L) is $V = Qt$, where Q is the dye solution flow rate. The theoretical estimations, according to the Bohart and Adams model, the N and K values are presented in Tables 1-9.

The effects of initial MB concentration have been investigated at 40-160 g·L^{-1}, respectively. The bed height was 15 cm and the temperature was 23 °C. The flow rate was fixed at 20 mL·min^{-1} and the pH of MB solution was 8. The breakthrough curves were plotted in figures (Figs. 1-20) according to the Bohart and Adams model. Flow rate is one of the most important characteristics in evaluating sorbents for continuous treatment of dyes effluents on an industrial scale [9, 10]. The effect of flow rate in the fixed bed column, packed with biomass, was investigated varying the flow rate from 10-40 mL·min^{-1} with bed depths held constant at 15 cm. The pH was 8. The influent MB

Table 1　Fixed bed column systems for spruce.

C_i	Q (mL/min)	x (cm)	m (g)	N	K	R	q_o (mg/g)
160	20	15	12	6,683	0.000318	-0.9506	40.99
160	20	15	12	7,400	0.000100	-0.9367	45.38
160	20	15	13	6,507	0.000356	-0.9992	36.84
160	20	15	13	6,387	0.000518	-0.9539	36.16
160	20	15	13	6,387	0.000518	-0.9539	36.16
160	20	15	15	5,329	0.000416	-0.9153	26.14
160	20	15	19	5,274	0.000415	-0.9457	20.16
160	20	15	19	5,274	0.000415	-0.9457	20.16
160	20	15	20	9,248	0.000110	-0.9530	19.19
160	20	15	20	8,738	0.000216	-0.9765	32.15
160	40	15	20	4,459	0.000515	-0.9903	16.41
160	40	25	34	5,320	0.000347	-0.9892	19.19
160	20	25	34	6,154	0.000243	-0.9870	22.20
80	40	25	34	4,480	0.000689	-0.9911	16.16

Table 2　Fixed bed column systems for spruce modified by autohydrolysis (x = 15 cm).

T (°C)	t (min)	C_i	Q (mL/min)	m (g)	N	K	R	q_o (mg/g)
160	0	160	20	16.5	9,643	0.000146	-0.9313	43.01
160	0	160	20	16.5	6,492	0.000541	-0.9651	28.96
160	20	160	20	16.5	6,362	0.000449	-0.9573	28.38
160	30	160	20	16.5	7,176	0.000381	-0.9325	32.01
160	40	160	20	16.5	6,092	0.000596	-0.9779	27.17
160	50	160	20	16.5	10,412	0.000193	-0.8966	46.44
180	10	160	20	16.5	6,926	0.000371	-0.9740	30.89
240	30	160	20	13.81	7,355	0.000229	-0.9551	41.06
240	50	160	20	14.16	5,389	0.000275	-0.9813	28.38

Table 3　Fixed bed column systems for pine (x = 15 cm).

T (°C)	t (min)	C_i	Q (mL/min)	m (g)	N	K	R	q_o (mg/g)
240	50	178	21	14.16	6,374	0.000220	-0.7944	25.87
		178	21	14.16	6374	0.000220	-0.7944	25.87

Table 4　Fixed-bed column systems for wheat straw.

C_i	Q (mL/min)	x (cm)	m (g)	N	K	R	q_o (mg/g)
160	20	15	4.4	-3,998	0.000100	-0.9396	6.43
160	40	15	14	-863	0.000083	-0.9245	6.21
160	20	25	22.6	4,053	0.000122	-0.9214	22.42
160	40	25	22.6	4,053	0.000122	-0.9214	22.42

Table 5　Fixed-bed column systems for barley straw.

C_i	Q (mL/min)	x (cm)	m (g)	N	K	R	q_o (mg/g)
160	40	15	20	4,221	0.000646	-0.9651	32.42
20	20	15	14	786	0.000793	-0.9413	6.07
20	20	15	5	72	0.001624	-0.9626	2.49
20	20	15	5	72	0.001624	-0.9626	2.49
160	40	15	20	2,052	0.000115	-0.8606	30.80
20	20	25	21.96	2,395	0.000450	-0.9698	10.90
160	40	15	22.6	6,264	0.000578	-0.9620	24.50

Table 6   Fixed-bed column systems for chickpea straw.

C_i	Q (mL/min)	x (cm)	m (g)	N	K	R	q_o (mg/g)
160	20	15	11	7,537	0.000139	-0.9829	50.43
160	20	15	11	7,559	0.000140	-0.9835	50.58

Table 7   Fixed-bed column systems for lentil straw.

C_i	Q (mL/min)	x (cm)	m (g)	N	K	R	q_o (mg/g)
160	10	15	9.03	5,310	0.00004	-0.9971	43.99
40	20	15	9	2,771	0.00019	-0.9901	22.66
160	10	15	9.03	2,822	0.00005	-0.9122	23.00
160	10	15	9.03	2,871	0.00005	-0.9086	23.40
80	20	25	15	7,666	0.00006	-0.9487	62.69
80	20	25	15	3,491	0.00010	-0.9588	31.24

Table 8   Fixed-bed column systems for algal biomass.

C_i	Q (mL/min)	x (cm)	m (g)	N	K	R	q_o (mg/g)
160	20	15	17	5,017	0.000124	-0.9548	22.76
160	40	25	28	2,509	0.000200	-0.9649	11.81

Table 9   Fixed-bed column systems for woodchips.

| C_i	Q (mL/min)	x (cm)	m (g)	N	K	R	q_o (mg/g)
160	20	15	6.5	-1,463	0.000208	-0.7523	6.51
160	20	15	8.6	-4,920	0.000131	-0.9360	4.84
160	40	25	14.6	-1,240	0.000175	-0.9599	5.90
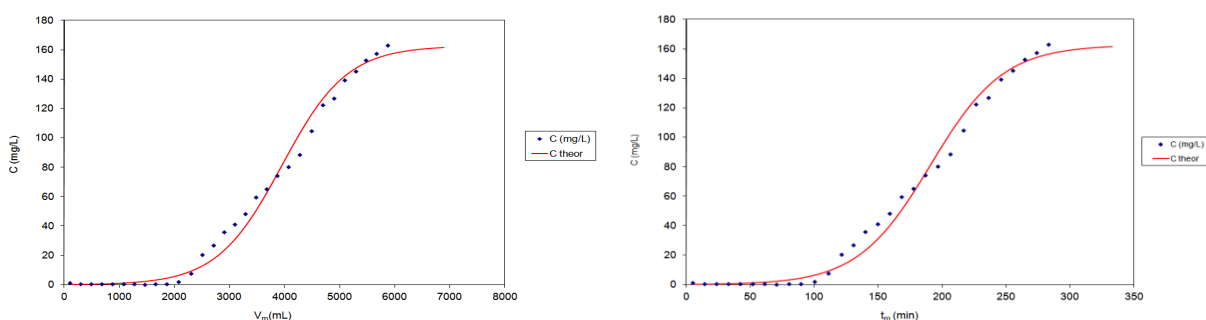
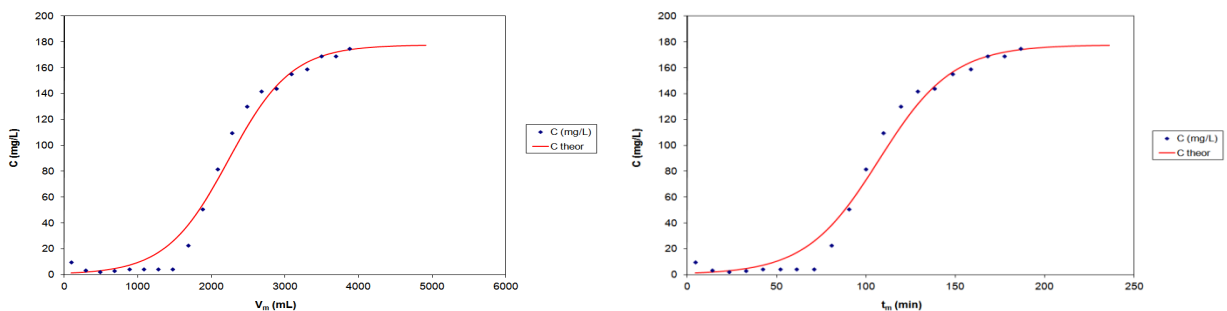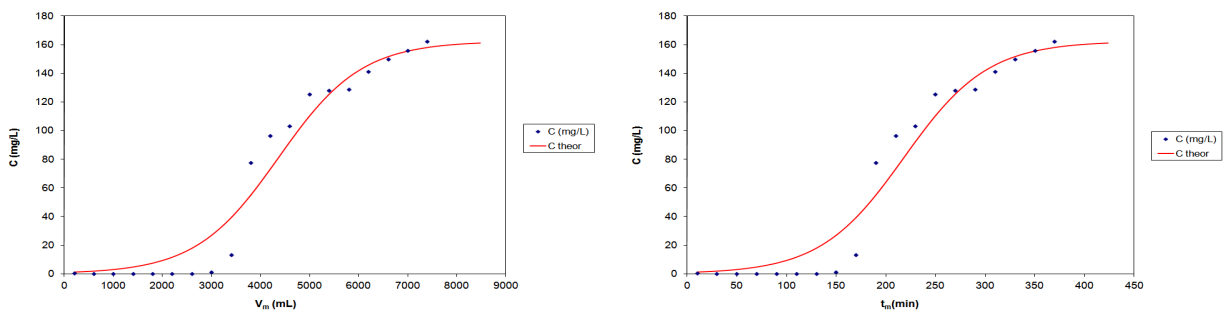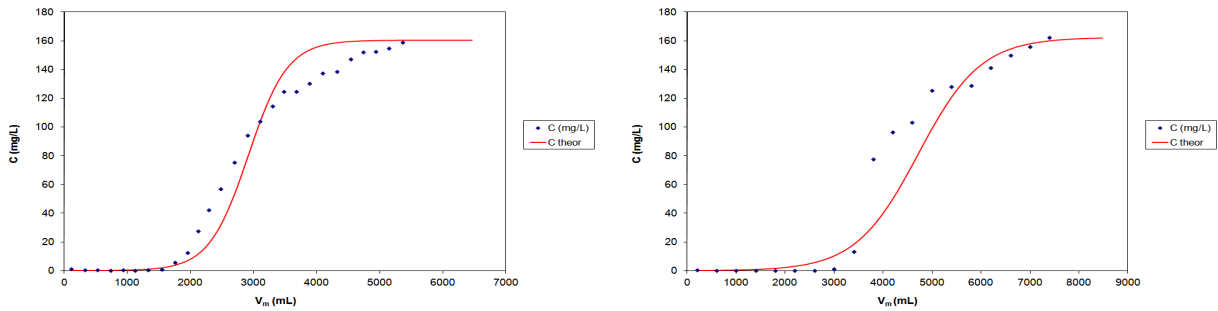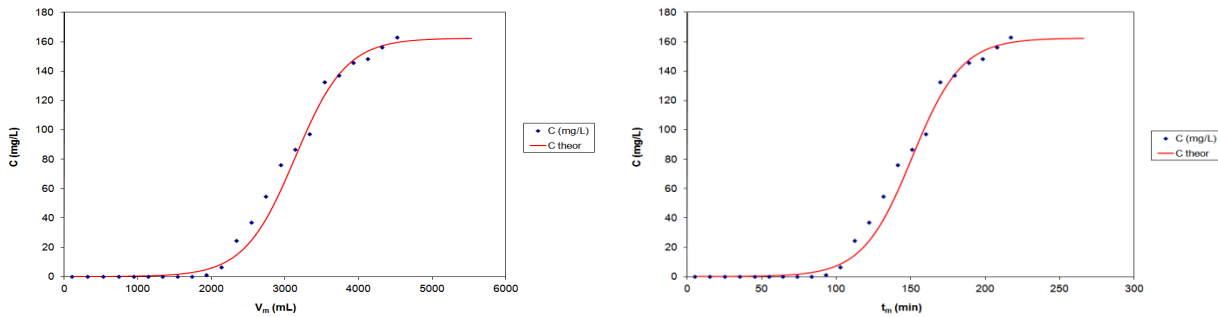**Fig. 1   Column experimental data and theoretical curves of MB adsorption on spruce; the effluent concentration is presented vs. (a) the effluent volume and (b) the adsorption time; $x = 15$ cm, $C_i = 160$ mg·L^{-1}, $Q = 20$ mL·min^{-1} (the theoretical curves are according to the Bohart and Adams model).**
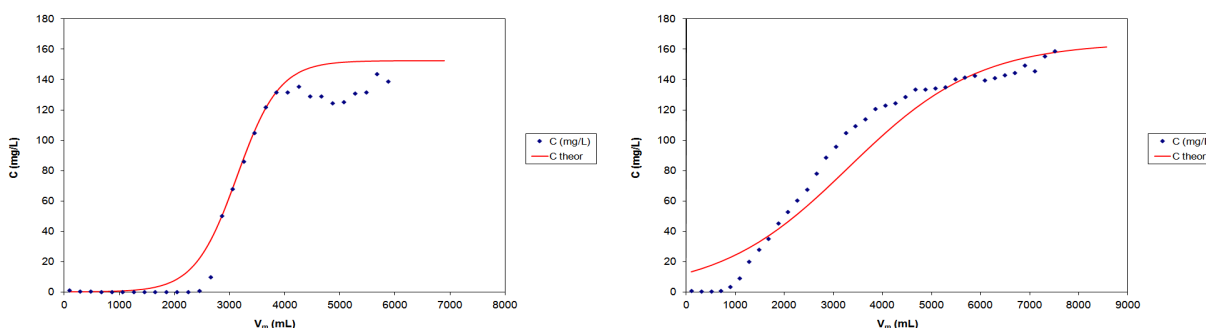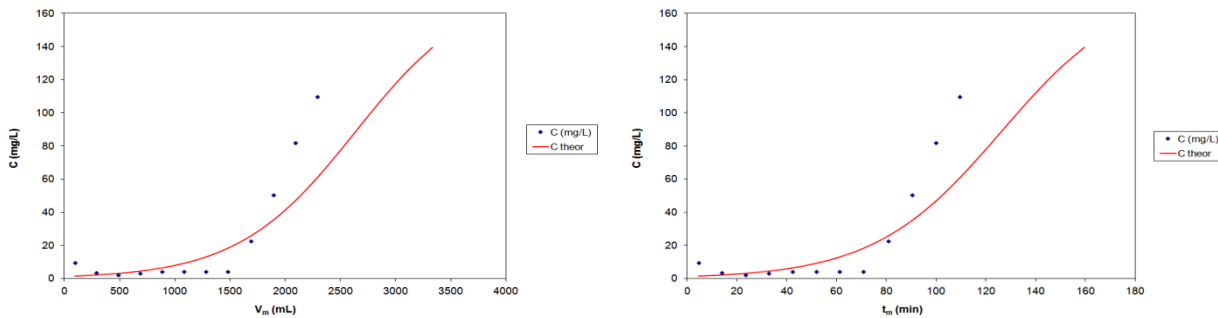

Fig. 2   Column experimental data and theoretical curves of MB adsorption on spruce; the effluent concentration is presented vs. (a) the effluent volume and (b) the adsorption time; $x = 15$ cm, $C_i = 160$ mg·L^{-1}, $Q = 40$ mL·min^{-1} (the theoretical curves are according to the Bohart and Adams model).
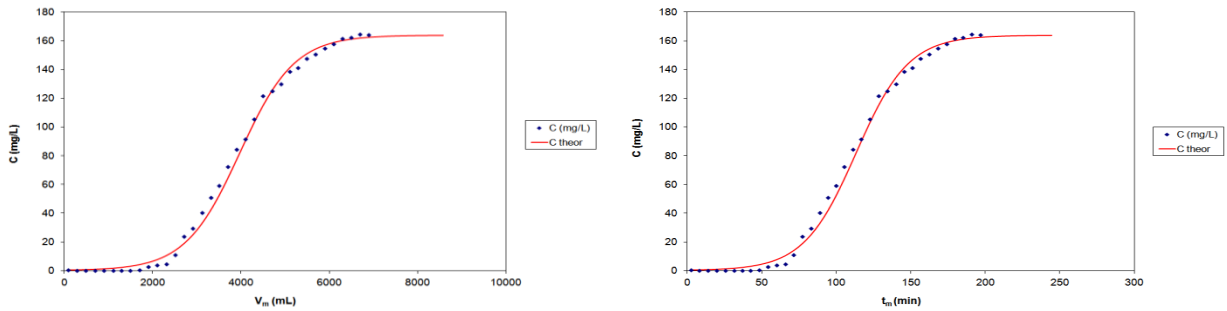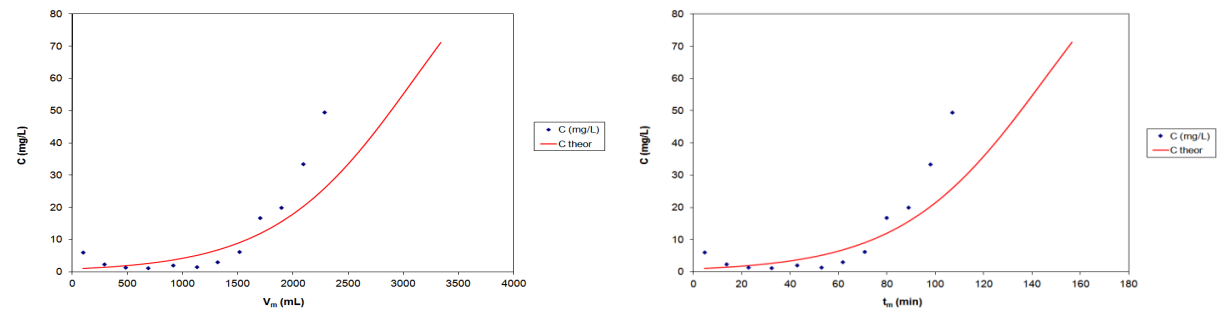
Fig. 3   Column experimental data and theoretical curves of MB adsorption on spruce; the effluent concentration is presented vs. (a) the effluent volume and (b) the adsorption time; $x = 25$ cm, $C_i = 160$ mg·L^{-1}, $Q = 40$ mL·min^{-1} (the theoretical curves are according to the Bohart and Adams model).
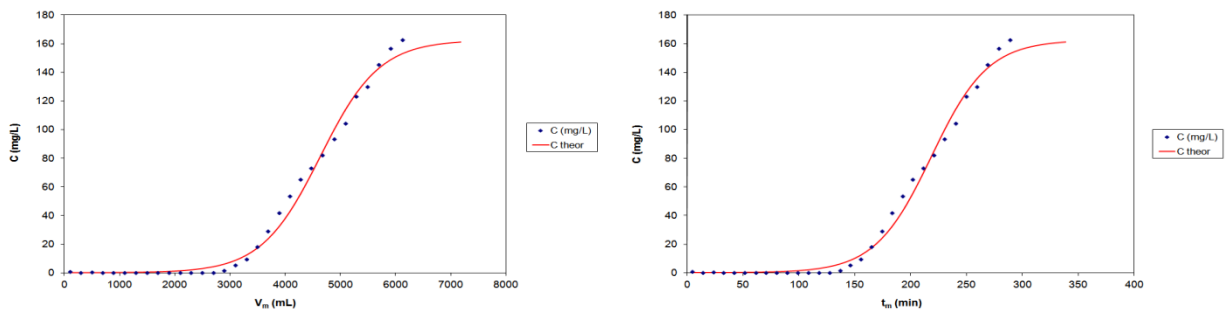
Fig. 4   Column experimental data and theoretical curves of MB adsorption on spruce; the effluent concentration is presented vs. (a) the effluent volume and (b) the adsorption time; $x = 25$ cm, $C_i = 160$ mg·L^{-1}, $Q = 20$ mL·min^{-1} (the theoretical curves are according to the Bohart and Adams model).

Fig. 5   Column experimental data and theoretical curves of MB adsorption on modified spruce; the effluent concentration is presented vs. (a) the effluent volume and (b) the adsorption time; $x = 15$ cm, $C_i = 160$ mg·L^{-1}, $Q = 20$ mL·min^{-1} (the theoretical curves are according to the Bohart and Adams model); modified by autohydrolysis at 240 °C for 0 min.

Fig. 6   Column experimental data and theoretical curves of MB adsorption on modified spruce; the effluent concentration is presented vs. (a) the effluent volume and (b) the adsorption time; $x = 15$ cm, $C_i = 160$ mg·L^{-1}, $Q = 20$ mL·min^{-1} (the theoretical curves are according to the Bohart and Adams model); modified by autohydrolysis at 240 °C for 30 min.

Fig. 7 Column experimental data and theoretical curves of MB adsorption on modified spruce; the effluent concentration is presented vs. (a) the effluent volume and (b) the adsorption time; $x = 15$ cm, $C_i = 160$ mg·L^{-1}, $Q = 20$ mL·min^{-1} (the theoretical curves are according to the Bohart and Adams model); modified by autohydrolysis at 160 °C for 50 min.

Fig. 8 Column experimental data and theoretical curves of MB adsorption on modified spruce; the effluent concentration is presented vs. (a) the effluent volume and (b) the adsorption time; $x = 15$ cm, $C_i = 160$ mg·L^{-1}, $Q = 20$ mL·min^{-1} (the theoretical curves are according to the Bohart and Adams model); modified by autohydrolysis at 180 °C for 10 min.

Fig. 9 Column experimental data and theoretical curves of MB adsorption on pine; the effluent concentration is presented vs. (a) the effluent volume and (b) the adsorption time; $x = 15$ cm, $C_i = 160$ mg·L^{-1}, $Q = 20$ mL·min^{-1} (the theoretical curves are according to the Bohart and Adams model).

Fig. 10 Column experimental data and theoretical curves of MB adsorption on pine; the effluent concentration is presented vs. (a) the effluent volume and (b) the adsorption time; $x = 25$ cm, $C_i = 160$ mg·L^{-1}, $Q = 20$ mL·min^{-1} (the theoretical curves are according to the Bohart and Adams model).
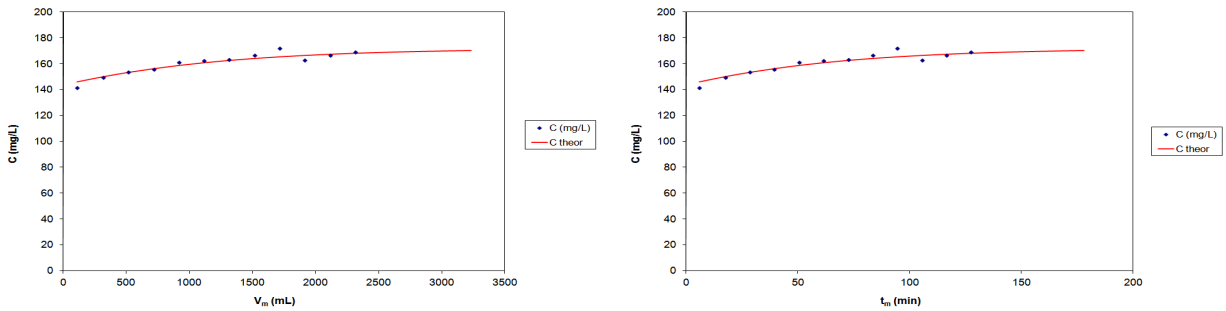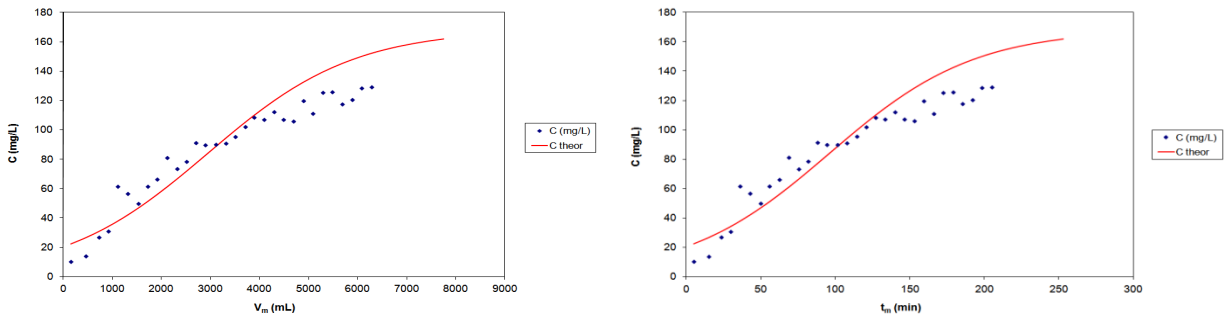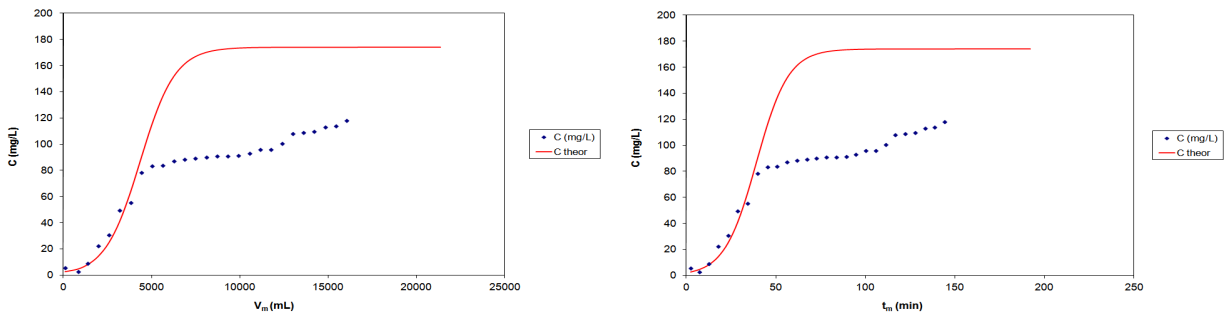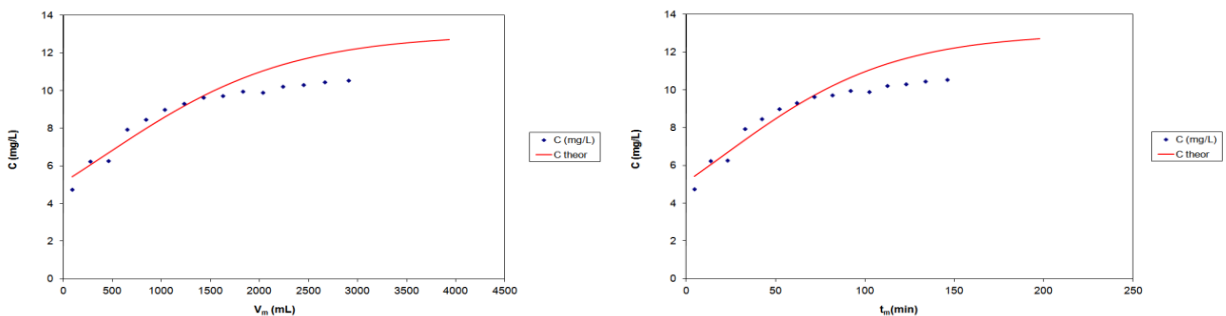
Fig. 11   Column experimental data and theoretical curves of MB adsorption on wheat straw; the effluent concentration is presented vs. (a) the effluent volume and (b) the adsorption time; $x = 15$ cm, $C_i = 160$ mg·L^{-1}, $Q = 20$ mL·min^{-1} (the theoretical curves are according to the Bohart and Adams model).

Fig. 12   Column experimental data and theoretical curves of MB adsorption on wheat straw; the effluent concentration is presented vs. (a) the effluent volume and (b) the adsorption time; $x = 25$ cm, $C_i = 160$ mg·L^{-1}, $Q = 40$ mL·min^{-1} (the theoretical curves are according to the Bohart and Adams model).
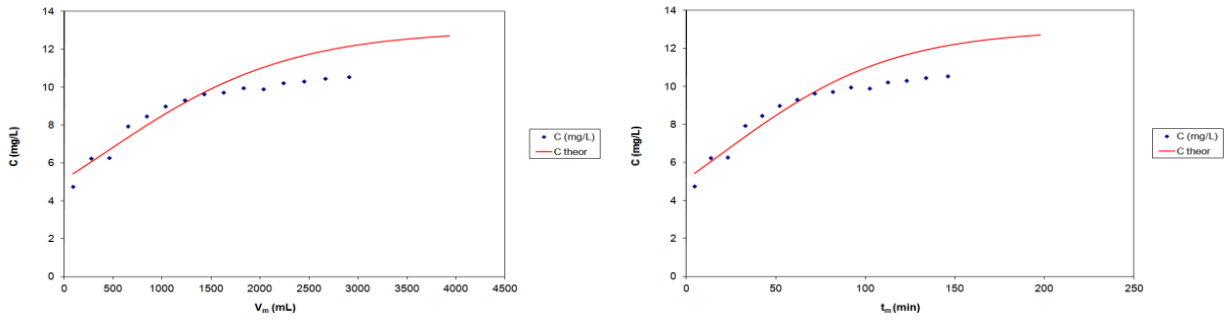

Fig. 13   Column experimental data and theoretical curves of MB adsorption on wheat straw; the effluent concentration is presented vs. (a) the effluent volume and (b) the adsorption time; $x = 15$ cm, $C_i = 160$ mg·L^{-1}, $Q = 40$ mL·min^{-1} (the theoretical curves are according to the Bohart and Adams model).
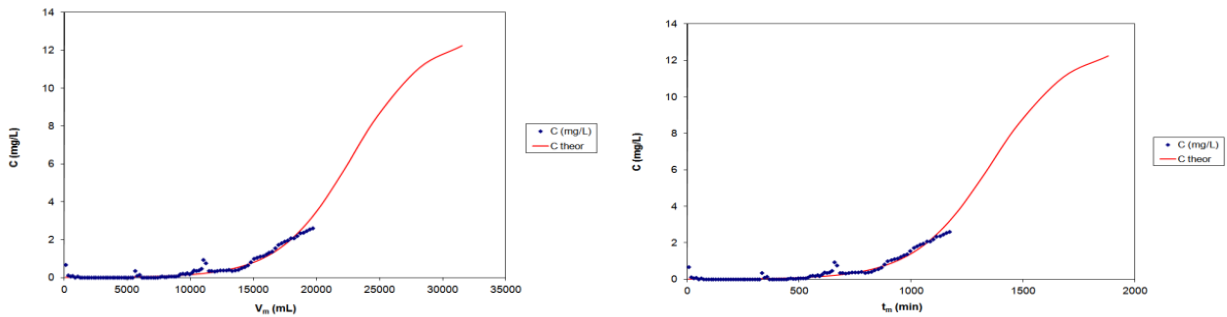

Fig. 14   Column experimental data and theoretical curves of MB adsorption on barley straw; the effluent concentration is presented vs. (a) the effluent volume and (b) the adsorption time; $x = 15$ cm, $C_i = 160$ mg·L^{-1}, $Q = 20$ mL·min^{-1} (the theoretical curves are according to the Bohart and Adams model).

Fig. 15   Column experimental data and theoretical curves of MB adsorption on barley straw; the effluent concentration is presented vs. (a) the effluent volume and (b) the adsorption time; $x = 15$ cm, $C_i = 160$ mg·L^{-1}, $Q = 20$ mL·min^{-1} (the theoretical curves are according to the Bohart and Adams model).

Fig. 16   Column experimental data and theoretical curves of MB adsorption on barley straw; the effluent concentration is presented vs. (a) the effluent volume and (b) the adsorption time; $x = 25$ cm, $C_i = 160$ mg·L^{-1}, $Q = 20$ mL·min^{-1} (the theoretical curves are according to the Bohart and Adams model).
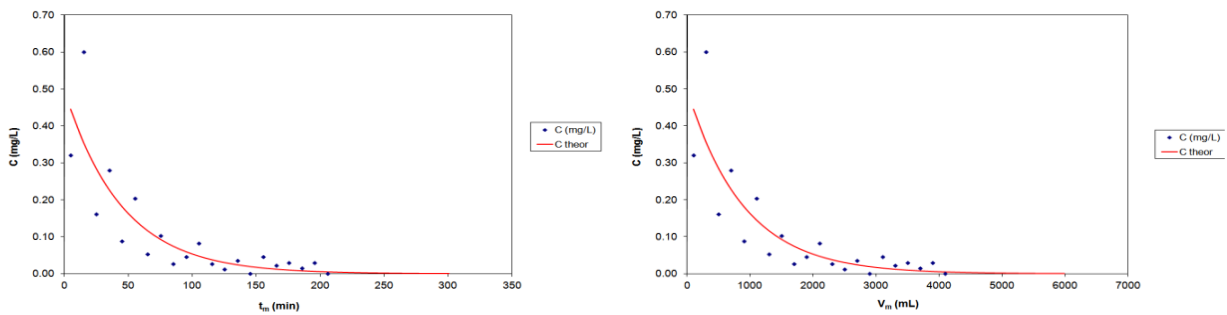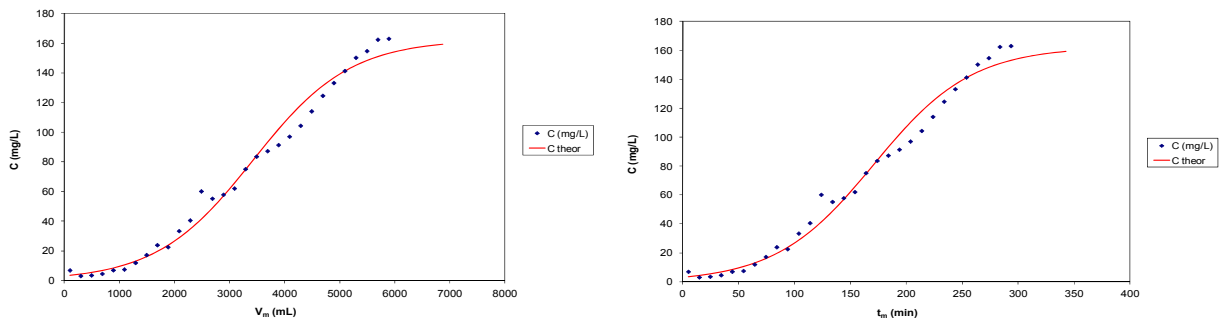

Fig. 17   Desorption of adsorbed at fixed-bed column system. Column experimental data and theoretical curves of MB adsorption on chickpea straw; the effluent concentration is presented vs. (a) the effluent volume and (b) the adsorption time; $x = 15$ cm, $C_i = 160$ mg·L^{-1}, $Q = 20$ mL·min^{-1} (the theoretical curves are according to the Bohart and Adams model).
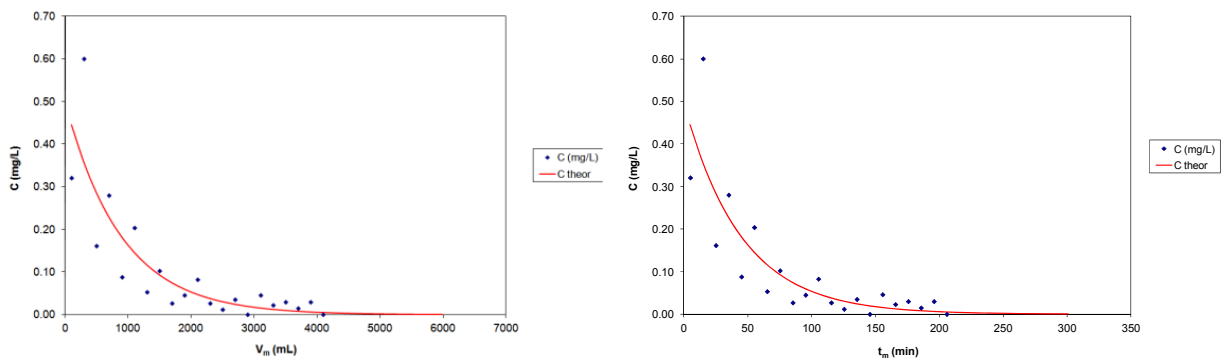

Fig. 18   Column experimental data and theoretical curves of MB adsorption on chickpea straw; the effluent concentration is presented vs. (a) the effluent volume and (b) the adsorption time; $x = 15$ cm, $C_i = 160$ mg·L^{-1}, $Q = 20$ mL·min^{-1} (the theoretical curves are according to the Bohart and Adams model).

concentration in the feed was 165 mg·L^{-1}. The adsorption capacity N was higher at lower flow rate values.

This could be explained by the fact that at lower flow rate, the residence of the adsorbate was longer and hence the adsorbent got more time to bind with the dye efficiently. In other words if the residence time of the solution in the column is not large enough for the adsorption equilibrium to be reached at the given flow rate, the dye solution leaves the column before the equilibrium occurs. It was observed that the adsorbent got saturated easily at higher flow rates. The MB uptake decreased with increase in flow rate. A decrease in flow rate increased the breakthrough time. The breakthrough curve was saturated earlier at higher flow rates because the front

of the adsorption zone quickly reached the top of the column. In contrast, lower flow rate and longer contact time, resulted in a shallow adsorption zone. In order to find the effect of bed height on the breakthrough curve, the adsorbate MB solution (initial MB concentration 165 mg·L^{-1}, pH 8) was passed through the adsorption column at a flow rate 70 mL·min^{-1} by varying the bed height. The results showed that the shape and gradient of the breakthrough curve was slightly different from the variation in the bed depth. The concentration of MB in the effluent rapidly increased after the breakthrough point. The lower bed depth (15 cm) gets saturated earlier than the higher bed depth (25 cm).

4. Desorption Results

Fig. 19   Column experimental data and theoretical curves of MB desorption from chickpeas straw; the effluent concentration is presented vs. (a) the effluent volume and (b) the desorption time; x = 15 cm, Q = 20 mL·min^{-1} (the theoretical curves are according to the Bohart and Adams model).
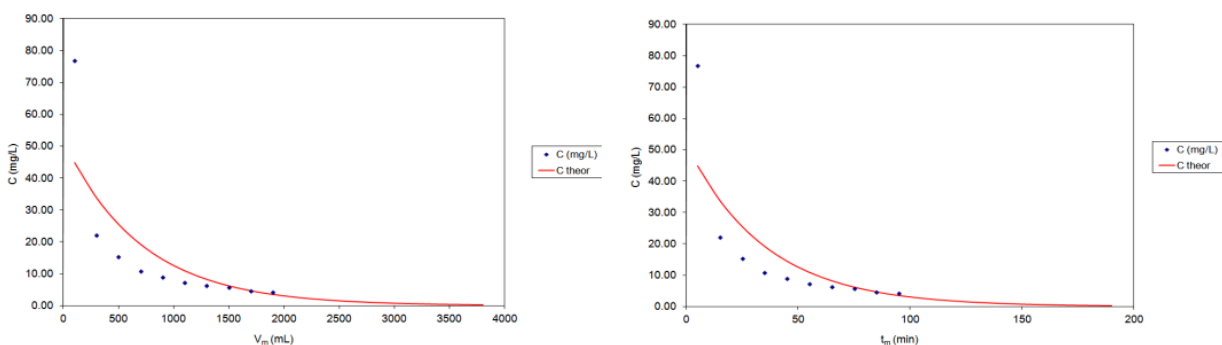
Fig. 20   Column experimental data and theoretical curves of MB desorption on wheat straw; the effluent concentration is presented vs. (a) the effluent volume and (b) the desorption time; x = 15 cm, Q = 20 mL·min^{-1} (the theoretical curves are according to the Bohart and Adams model).

References

[1] Lee, J. M., Shi, J., Venditti, R. A., and Jameel, H. 2009. "Autohydrolysis Pretreatment of Coastal Bermuda Grass for Increased Enzyme Hydrolysis." *Biores. Techn.* 100 (24): 6434-41.

[2] Nabarlatz, D., Ebringerová, A., and Montané, D. 2007. "Autohydrolysis of Agricultural By-Products for the Production of Xylo-Oligosaccharides." *Carbohyd. Polym.* 69 (1): 20-8.

[3] Shukla, A., Zhang, Y.-H., Dubey, P., and Margrave, J. L. 2002. "The Role of Straw in the Removal of Unwanted Materials from Water." *J. Hazard. Mater. B* 95: 137-52.

[4] Crini, G. 2006. "Non-conventional Low-Cost Adsorbents for Dye Removal: A Review." *Biores. Technol.* 97 (9): 1061-85.

[5] Gupta, V. K. 2009. "Application of Low-Cost Adsorbents for Dye Removal—A Review." *J. Env. Manag.* 90: 2313-42.

[6] Gupta, V. K., Carrott, P. J. M., and Ribeiro Carrott, Suhas, M. M. L. 2009. "Low-Cost Adsorbents: Growing Approach to Wastewater Treatment—A Review." *Cr. Rev. Env. Sc. Techn.* 39: 783-842.

[7] Demirbas, A. 2009. "Agricultural Based Activated Carbons for the Removal of Dyes from Aqueous Solutions: A Review." *J. Hazard. Mater.* 167: 1-9.

[8] Rafatullaha, M., Sulaiman, O., Hashim, R., and Ahmad, A. 2010. "Adsorption of Methylene Blue on Low-Cost Adsorbents: A Review." *J. Hazard. Mater.* 177: 70-80.

[9] Nigam, P., Armour, G., Banat, I. M., Singh, D., and Marchant, R. 2000. "Physical Removal of Textile Dyes from Effluents and Solid-State Fermentation of Dye-Adsorbed Agricultural Residues." *Biores. Technol.* 72: 219-26.

[10] Batzias, F. A., and Sidiras, D. K. 2004. "Dye Adsorption by Calcium Chloride Treated Beech Sawdust in Batch and Fixed-Bed Systems." *J. Hazard. Mater. B* 114: 167-74.